An Investigation of Downcomer Boiling Effects During Reflood Phase Using TRAC-M Code

Woochong Chon*, Jae-Hoon Lee, Sang-Jong Lee
Safety Analysis Dept., Korea Nuclear Fuel Co., Ltd.,
493 Deokjin-dong, Yuseong-gu, Daejeon 305-353, Korea

The capability of TRAC-M code to predict downcomer boiling effect during reflood phase in postulated PWR LOCA is evaluated using the results of downcomer effective water head and Cylindrical Core Test Facility (CCTF) experiments, which were performed at JAERI. With a full height downcomer simulator, effective water head experiment was carried out to investigate the applicability of the TRAC-M best estimate LOCA code to evaluate the effective water head with superheated wall temperature in downcomer. In order to clarify the effect of the initial superheat of the downcomer wall on the system and the core cooling behaviors during the reflood phase, two sets of analysis were also performed with a CCTF. Results show that TRAC-M code tends to under-predict downcomer effective water head and core differential pressure. However, the code results show a good agreement with the experimental results in downcomer temperature, heat flux and pressure. Finally, both experiment and calculation showed that the downcomer water head with the superheated downcomer wall is lower than that of the saturated wall temperature.

Key Words : Downcomer Boiling, LOCA, Reflood, TRAC-M, Effective Water Head, CCTF

Nomenclature

C : Drag Coefficient
D_h : Hydraulic Diameter
f : Friction Factor
T : Temperature
V : Velocity
α : Gas volume fraction
α_w : Wall void fraction
ρ : Density of fluid

Subscripts

ag : Agitated inverted annular flow to post agitated transition
d : Droplet
dd : Dispersed droplets
df : Highly dispersed flow
fr : Free stream bubbles
g : Combined gas mixture
i : Interfacial
l : Liquid
pa : Post agitated flow
r : Relative
rw : Rough wavy inverted annular flow
sat : Saturation
sb : Subcooled boiling
sm : Smooth inverted annular flow
v : Water vapor
w : Wall

* Corresponding Author,
E-mail : wcchon@knfc.co.kr
TEL : +82-42-868-1849; **FAX** : +82-42-863-4430
Safety Analysis Dept, Korea Nuclear Fuel Co, Ltd., 493 Deokjin-dong, Yuseong-gu, Daejeon 305-353, Korea. (Manuscript **Received** October 25, 2004; **Revised** March 29, 2005)

1. Introduction

The issue of downcomer boiling was first reported in 2000. Downcomer boiling is caused by the metal heat release from vessel and core barrels walls to fluid in the downcomer gap. Metal heat from the vessel lower head and structures in the lower plenum also contribute to downcomer boiling. As heat is released to the downcomer fluid,

fluid temperature is gradually increased and eventually subcooled and saturated boiling takes place. Voids generated by these processes displace water in the downcomer and reduce the water head which is the only driving force to supply emergency core coolant into core during reflood phase in a large cold leg break loss of coolant accident (LBLOCA). This loss in driving force can significantly reduce the core flooding rate, and allowed a prolonged secondary heat-up to take place. Hence, it is necessary to understand clearly the physical phenomenon of downcomer boiling during reflood phase.

Evaluation Models based on Appendix K do not necessarily capture this phenomenon, since nodalization of the downcomer and modeling of subcooled boiling is simplified in those types of Evaluation Model codes. This prohibits the code from calculating thermal stratification for the entire vessel component. Previous experimental and numerical studies have shown that the neglect of downcomer boiling during reflood in a large break loss of coolant accident could be a non-conservative assumption.

The effect of the highly heated wall on the downcomer was studied by Sudo and Akimoto (1982). with the test facility modeling the downcomer part of the actual PWR system. They confirmed experimentally that the static water head was decreased because of the steam generation due to the heat release from the superheated slab. They developed a correlation to evaluate the void fraction in the downcomer and studied the effect of the scaling factor and the applicability of the correlation for the prediction of the static water head. The effect of the initial superheat of the downcomer wall on the system behavior was studied by Akimoto and Murao using the Cylindrical Core Test Facility (Akimoto and Murao, 1983). They concluded that the initial superheat of the downcomer wall resulted in the lower downcomer water head and caused the core inlet subcooling to be decreased, and led to the lower core water head. However results showed the difference of core inlet mass flow rate was small between the superheated and the saturated wall tests since the loosing mass flow rate through the intact loops was compensated by the mass flow rate through the broken loop.

Since downcomer boiling is the one of the new issues concerned in nuclear power plant recently, not many researchers have attempted to perform an analytical study. For this reason, almost no open literature about analytical study is available in downcomer boiling issue.

The purpose of this study is to investigate the capability of TRAC-M code to predict downcomer boiling effect during reflood phase in postulated PWR LOCA (Steinke et al., 2001). The first downcomer simulation model is composed of two flat plates located in parallel to simulate the rectangular downcomer flow channel and has three regions simulating a lower plenum, effective heated region and upper annulus. Two different geometries, Cylindrical and Cartesian, are applied in simplified downcomer simulation model. And also sensitivity study for different nodalization was done. The second applied model is CCTF Core 1 which is an experimental facility designed to model Westinghouse 4-loop PWRs. It is a full-height test facility built and operated by JAERI. Cylindrical coordinate system is used in CCTF model and calculations are done for both superheated and saturated downcomer wall tests. The database obtained from the current research can be the groundwork for the future studies about downcomer boiling issue.

2. Description of Works

2.1 Test facilities description

Experimental investigation of downcomer boiling is very limited. Most reflood test facilities have been designed for low pressure operation. Two experimental tests, which are the most corresponding to the downcomer boiling issue up to date, were selected in current study. These are downcomer effective water head test and Cylindrical core test facility (CCTF) experiments.

2.1.1 Downcomer effective water head test

Downcomer effective water head test was performed by Sudo and Akimoto in 1981.(Spore et al., 2001 ; Sudo and Akimoto, 1982) The objec-

tives of this test are to investigate the effect of the predominant parameters on the effective water head and also to check the availability of their correlation for predicting the effective water head. The superheated wall temperature test data was selected from many other different boundary conditions to simulate downcomer boiling effect. A schematic view of test facility is shown in Fig. 1 (Sudo and Akimoto, 1982). The downcomer simulator is made of two carbon steel flat plates located in parallel to make up the rectangular downcomer flow channel, whose dimension is also given in Fig.1. The gap of flow channel is changeable from 0.05 to 0.2 m, however fixed 0.2 m gap test is chosen for current study since it is a realistic width of downcomer. The downcomer simulator is composed of three regions simulating a lower plenum, effective heated region and upper annulus. The lower plenum region and the upper annulus region are unheated. The effective heated region is 5.0 m in height and heaters are attached on the outer surfaces in the effective heated region in order to heat the walls up to 300℃.

Actual downcomer walls of a typical PWR have stainless steel cladding on the inner surfaces. Therefore, cladding is required to properly simulate histories of heat release from walls into fluid and besides, prevents the erosion of carbon steel by water during tests. The dimensions of two flat plates are 0.05 m in thickness of carbon steel plate and 0.006 m in thickness of stainless steel cladding. In order to inject emergency core coolant, two water supply lines are provided to the downcomer simulator. The initial injection line is used to establish two phase mixture over the downcomer flow channel as fast as possible by injecting water with a high flow rate at the bottom of the downcomer. On the other hand, LPCI line is used to simulate the cold leg injection by injecting water at the top of the effective heated region of the downcomer. A water overflow line is provided at the top of the effective heated region of the downcomer. In case of current test, the velocity of injected water through the initial injection line at the lower plenum is 0.2 m/s for initial 30 sec and 0.035 m/s from the LPCI line after that.

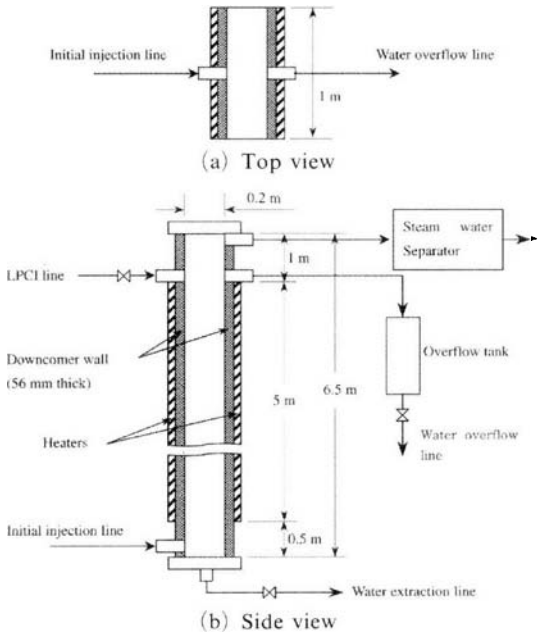

Fig. 1 Schematic view of effective downcomer water head experiment facility

As for the instruments, 25 sets of thermocouples and 11 differential pressure transducers are equipped at different elevations of downcomer walls. A set of thermocouples is composed of three thermocouples, which are located at 0, 8 and 51 mm apart from the inner surface in the wall at each elevation.

2.1.2 Cylindrical core test facility (CCTF) test

The CCTF was designed to reasonably simulate the flow conditions in the primary system of a four loop PWR during the refill and reflood phases of a LOCA (Boyack et al., 1998 ; Akimoto and Murao, 1983). The reference reactors are the Trojan reactor and, in certain aspects, the Ohi reactor in Japan. The vertical dimensions and the flow paths of the system components in the CCTF are kept as close to the reference reactor as possible. The flow area of each system component is scaled down in proportion to the scaling factor of the core flow area, that is, 1/21.4. The assumed break location is the cold leg piping corresponding to the outer surface of the biological shield of the reference reactor.

The CCTF facility is equipped with four primary loops, which are composed of three intact loops and a broken loop. Each loop has a hot-leg-piping section, an active steam generator, a loop-seal-piping section, a pump simulator, an emergency core cooling (ECC) injection port and a cold-leg-piping section. The emergency core cooling system (ECCS) of the CCTF consists of the accumulator (ACC) and LPCI systems. Each system is connected to the ECC water injection ports attached at the cold legs and the lower plenum of the pressure vessel. Figure 2 shows the schematic view of CCTF.

The core consists of 32 bundles arranged in a cylindrical configuration. Each bundle consists of 8×8 heater rods and it contains 57 heater rods and 7 non-heated rods. The 57 heater rods consist of 12 high, 17 medium and 28 low power rods. The power ratios of the high, medium and low power rods to the bundle-average power are 1.1, 1.0 and 0.95, respectively. The radial dimension of each internal is scaled down by factor of 8/15 from that of the reference reactor because the heater rods of the CCTF simulate the 15×15 array fuel assembly. The downcomer is an annulus with 0.0615 m gap in the CCTF. In the scaling of the CCTF downcomer, the volume of the baffle region in the reference reactor was added to the volume of the downcomer. The CCTF has a wider downcomer gap. However, the wider downcomer provides more conservative water accumulation rate in the downcomer. The outside wall of the downcomer is constructed of carbon steel cladded with 0.005 m stainless steel. The thickness of carbon steel is 0.085 m. The wall is preheated to a certain temperature before the test.

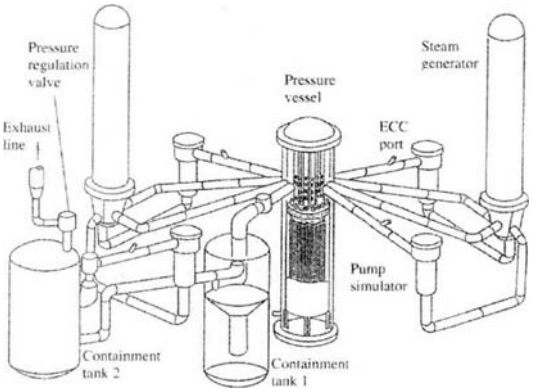

Fig. 2 Perspective schematic of CCTF

Two experiments were conducted which provide a sensitivity relevant to downcomer boiling. The first test was performed with the downcomer wall initially superheated. The initial temperature was 460 K to provide approximately 70 K initial superheating. The other test was performed with the downcomer wall initially at the saturation temperature of 388 K.

2.2 TRAC-M code modeling

2.2.1 Downcomer effective water head test

To simulate the current test, TRAC-M F90 Ver. 3.782 code has been used (Steinke et al., 2001). This test loop is modeled using 9 Components including 2 Heat Structure SLABs, and 6 Junctions. The downcomer simulator is modeled as a Vessel Component without reactor-core region in 3D Cartesian coordinate as shown in Fig 3. The 12 axial cells are set with considering the position of temperature sensors installed on the downcomer simulator plates. One initial injection inlet pipe is connected with level 1 and LPCI inlet pipe and overflow outlet pipe are connected with level 12. The total cell number is 2 in X-direction and 1 in Y-direction. Each Heat Structure SLAB Component is applied to the heating wall with 5 node points for the measurements of wall temperature distribution in X-direction. The position of node points was set for the comparison of data with experiment. The boundary condition for the inner surface of the Heat Structure SLAB element is coupled to the specified cells in hydraulic Vessel Component and the outer surface of the SLAB is set as an adiabatic boundary condition. The initial wall temperature is set on 523 K. Injection time is controlled by TRIP and time based mass flow rate table given in FILL Components to match the same boundary conditions with experiment. The initial pressure is set on 1 atm. The Blasius interfacial drag correlation is applied in the lower plenum and downcomer of VESSEL Component. In addition, Cylindrical coordinate is tested for the comparison. The calculation is

also performed with the axial cell number change to 19 and 31 for the evaluation of node sensitivity. Test conditions, properties and dimensions used in calculation are the same as experiment and important test conditions are given in Table 1.

The effect of break is not considered in this modeling since the main purpose of the downcomer effective water head test is to confirm the ability of wall to liquid heat transfer analysis with superheated wall temperature using TRAC-M. This investigation results provided the basic analysis information of boiling occurring in downcomer simulator.

Table 1 Test conditions for downcomer water head test

Test Condition	Input
System Pressure (Pa)	1.0E+05
Downcomer Wall Temp. (K)	523
ECC Liquid Temp. (K)	372
Initial Injection Rate (m/s)	0.2
LPCI Rate (m/s)	0.035

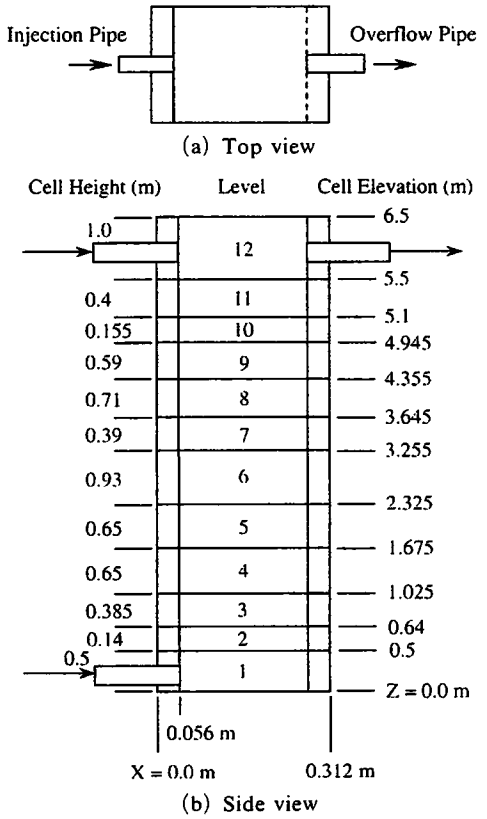

Fig. 3 Vessel nodalization for effective downcomer water head test

2.2.2 CCTF superheated/saturated wall temperature test

The CCTF test loop is modeled using 53 Components, 31 Junctions and 24 Heat Structures. In TRAC-M code, the pressure vessel is modeled in 3D Cylindrical coordinate as shown in Fig. 4. The pressure vessel is divided into 22 axial levels, four radial rings and four azimuthal sectors for a total of 352 fluid cells for a reactor nodalization. The fourth ring from the core center simulates downcomer area. The lower plenum nodding contains three axial levels. For the code to adequately model the sweep-out effect, other analyses have

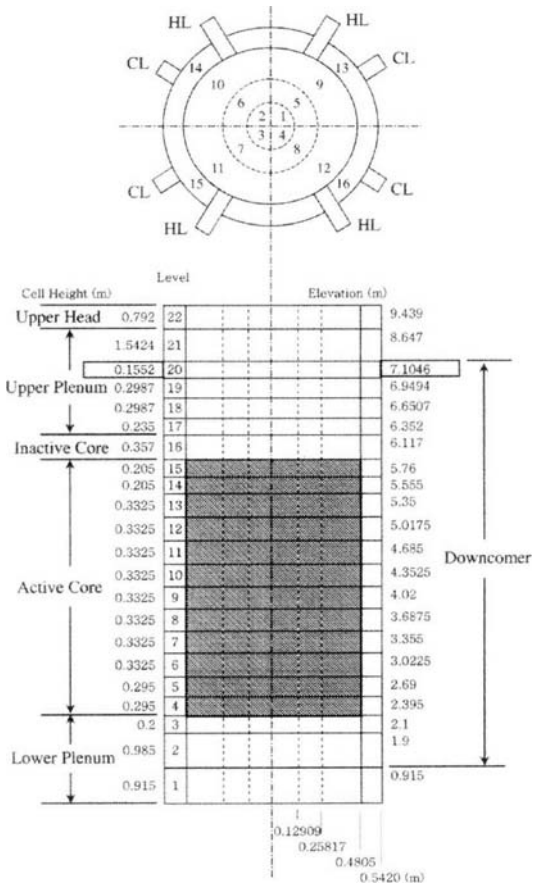

Fig. 4 Vessel nodalization for CCTF test

Table 2 Test conditions for CCTF superheated and saturated wall temperature tests

Test Conditions	Superheated	Saturated
Total Power (MW)	9.36	9.35
System Pressure (MPa)	0.211	0.208
Containment Pressure (MPa)	0.2	0.2
Initial Downcomer Wall Temp. (K)	460	388
ECC Liquid Temp. (K)	312	311
Accumulator Flow Rate (m^3/s)	0.0672	0.07

shown that at least two cells are required below the downcomer skirt. The upper plenum is defined as the region between the top of the active core and the bottom of the upper head. From the outlet of the active core to the nozzle region, four cells are defined. Level 22 represents upper head area. The hot and cold legs are connected to level 20. The heater rods are located from level 4 to level 15 and total length is 3.66 m. Accumulator and LPCI injection times are controlled by flow rate tables given in FILL Components to set the same conditions with experiment. The main test conditions are given in Table 2.

All four loops are modeled identically except loop 4 contains the cold leg break between the pump simulator and reactor vessel. Each loop models the hot leg piping, steam generator primary and secondary fluid volume and heat transfer. Each loop also contains modeling of the accumulator and high and low pressure injection ECCSs. The hot leg connects the reactor vessel to the steam generator inlet plenum. The hot leg is modeled with a TEE Component to allow for the connection of the pressurizer surge line. The primary tube of the TEE is modeled identically to the PIPE Components in the other loops. The U-tubes are modeled for the boiling region of the steam generator. The dominant phenomena needed to capture are steady state heat balance and steam binding during reflood phase. The pump discharge cold leg region is modeled with a TEE Component. The secondary tube of the TEE provides for ECC injection.

The core consists of three radial rings, which have different power ratios of the high, medium and low power RODs. The average powers are 1.158, 1.080 and 0.885, respectively. The time dependent ROD power decay is given by table in ROD component, which is obtained from experiment data.

2.2.3 TRAC-M reflood interfacial drag coefficient

The interfacial drag is the one of main factors effecting on downcomer boiling during reflood phase. TRAC provides separate interfacial drag models for each of the flow regimes. In terms of interfacial drag, the overall interfacial drag coefficient for a given hydraulic cell is defined as the weighted average of the individual reflood flow regime drag coefficients. Throughout the regimes of subcooled nucleate boiling, nucleate boiling, and transition boiling, TRAC applies the subcooled boiling interfacial drag model. Specifically, if $T_l \geq T_{sat}$

$$C_{i,sb}=\frac{C_{i,w}V_l^2+ffs\cdot C_{i,fr}\cdot V_r^2}{(\alpha_w+\alpha_{fr})V_r^2} \tag{2}$$

for $\alpha_w>0$, and

$$C_{i,sb}=\frac{ffs\cdot C_{i,fr}}{\alpha_{fr}} \tag{3}$$

for $\alpha_w\leq 0$, where the numerical factor $ffs=0.00125$ (Spore et al., 2001).

In the smooth inverted annular flow regime,

$$C_{i,sm}=2\rho_g f_{i,sm}\frac{(1-\alpha_g)^{1/2}}{D_h} \tag{4}$$

where $f_{i,sm}$ is calculated from the smooth tube friction factor relations (Spore et al., 2001).

The interfacial drag coefficient for rough wavy inverted annular flow is identical to that of the

smooth inverted annular flow regime, with the exception of the friction factor $f_{i,rw}$, which is evaluated from the Colebrook equation for fully turbulent flow over rough surfaces.

$$C_{i,rw}=2\rho_g f_{i,rw}\frac{(1-\alpha_g)^{1/2}}{D_h} \tag{5}$$

In the agitated inverted annular flow regime, the interfacial drag coefficient is defined by

$$C_{i,ag}=C_{i,rw} \tag{6}$$

and in the post agitated flow regime, $C_{i,pa}$ is calculated as a weighted average of the rough wavy and highly dispersed flow drag coefficients.

The highly dispersed flow regime is characterized by small liquid droplets distributed throughout the vapor and by liquid films that may form on unheated surfaces based on the work of Cappiello (1989),

$$C_{i,df}=\frac{C_{i,dd}V_r^2+C_{i,f}V_V^2}{\left(V_V-\frac{\alpha_{dd}V_d}{1-\alpha}\right)^2} \tag{7}$$

The dispersed droplet drag coefficient is given by,

$$C_{i,dd}=fcdrop\frac{0.75\alpha_{dd}\rho_g C_d}{d_d} \tag{8}$$

where the numerical factor $fcdrop$=0.015 (Spore, 2001).

3. Results

3.1 Downcomer effective water head test

3.1.1 Comparison of wall temperature

The transient calculations were performed in current analysis since downcomer effective water head test was done with only transient conditions. The wall temperature histories are compared between experiment and calculation before other comparisons since wall temperature is a major factor affecting on the boiling and water head in this test. Figure 5 shows the comparison of wall temperature histories between experiment and calculation at the 0.85 m height from the bottom of heated region. Three different distances of 0, 8 and 51 mm from the inner surface of downcomer simulator plate are set for the temperature measurement using thermocouples at the same elevation. The node points are also set at the same locations as experiment to obtain wall temperature distribution in TRAC analysis model. The temperature trends of calculation result are very similar to experiment with same boundary conditions. The temperature differences between calculation and experiment are shown at the beginning of water injection period, since water level is not exactly flat during the water injection in experiment. And other temperature differences inside wall seems due to the different effect of conduc-

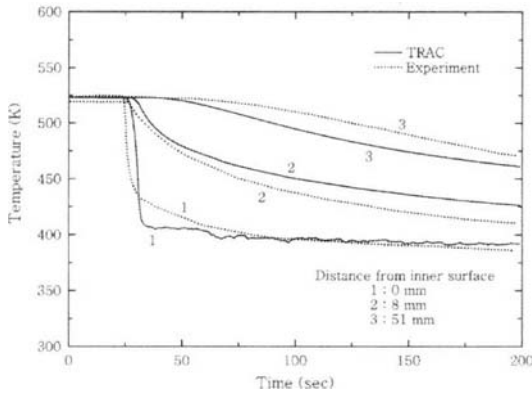

Fig. 5 Comparisons of temperature histories between experiment and calculation (Hight from the Bottom of Heated Region : 0.85 m)

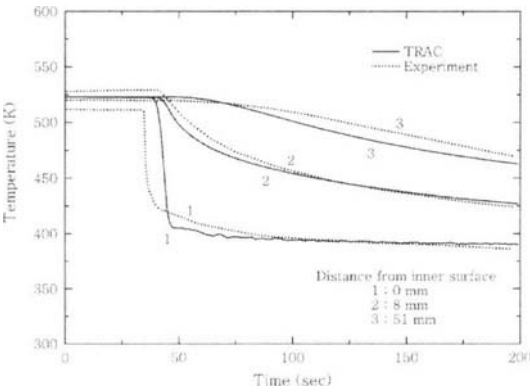

Fig. 6 Comparisons of temperature histories between experiment and calculation (Hight from the Bottom of Heated Region : 4.15 m)

tion during measuring process using thermocouples in experiment. Figure 6 shows the comparison of wall temperature histories at the 4.15 m height from the bottom of heated region. It also shows good agreements except at the period of water injection started since the injection starting time is not exactly same as that of experiment. The small temperature differences at the beginning of experiment are also shown in this figure, since steady state condition may not be achieved during temperature measurement.

3.1.2 Comparison of pressure difference

Figure 7 shows the comparisons of pressure difference between experiment and calculation at the elevations of 0~0.685, 0~1.675 and 0~4.645 m from the bottom of heated section. TRAC result shows the maximum pressure differences are matched well with experimental results and average pressure differences are lower than those of experimental result. It also shows the trend of pressure difference is similar with experimental result. The following three characteristic regions can be identified in this figure according to the pressure difference change rate (dP/dt) variation.

Region 1 : Pressure differences are increasing rapidly from the initiation of water injection for about 20 seconds. Increasing rate of water head corresponds to the velocity of water injected by the initial injection line.

Region 2 : Pressure differences are decreasing from the maximum to the minimum for about 50 seconds in this period (50~100 sec after water injection).

Region 3 : Pressure differences are again increasing slowly to the almost constant value after 100 seconds from the initial water injection.

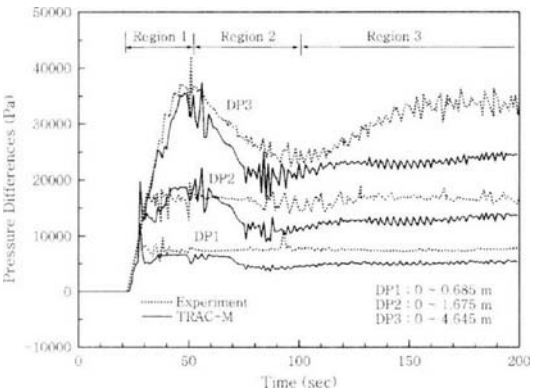

Fig. 7 Comparison of differential pressure between experiment and calculation

The occurrence of Region 1 is intimately related to the velocity of water injection. The Region 1 corresponds to the period of initial injection line actuated. In this period, overall pressure difference is increasing with almost the same rate as the flow rate given by the initial injection line. The time at the maximum pressure difference corresponds to the time when the water injected through the initial injection line starts to flow out through the overflow pipe line and injection is switched to the LPCI line from the initial injection line.

The occurrence of Region 2 may be pointed out that flow rate of steam generated in the downcomer is increasing along with the progression of the quench front from the bottom to the top of the downcomer walls during Region 1. There should be some time lag for generated steam to accumulate upwards and to escape from the top of the heated region. The pressure difference of Region 3 is increasing slowly since the heat released from the walls is decreasing in this period. The TRAC calculation results tend to under-predict downcomer water head at various elevations in Region 3. It means that TRAC calculate the lager boiling effect in downcomer simulator than that of experiment. However the difference is small and is in conservative range.

3.1.3 History of heat flux and sensitivity study

Figure 8 shows the comparison of heat flux calculated from temperature history of experimental result with data calculated. It shows that there is no serious discrepancy between the experiment and the calculated and most of data points are located within 10% error range. The data points, which are the out of 10% error range, are mainly caused from initial water/wall temperature differences between experiment and cal-

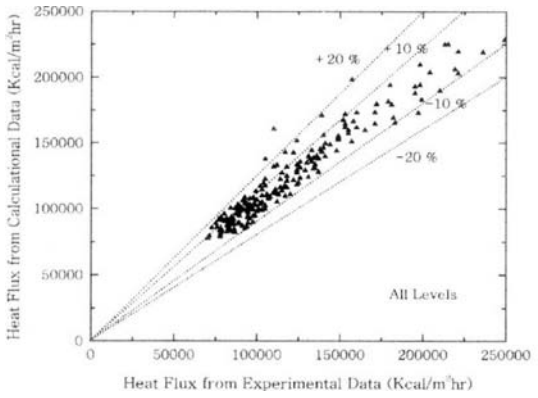

Fig. 8 Comparison of heat flux between experiment and calculation

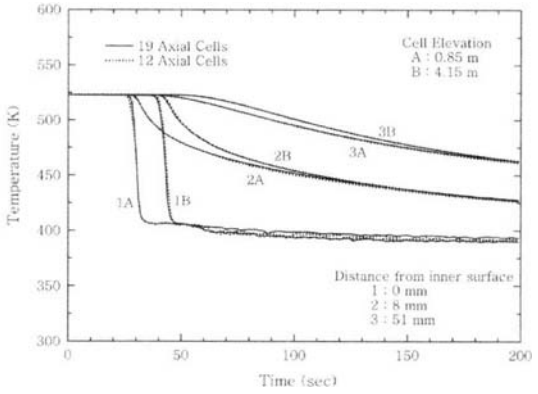

Fig. 10 Comparisons of temperature histories for different axial cell numbers

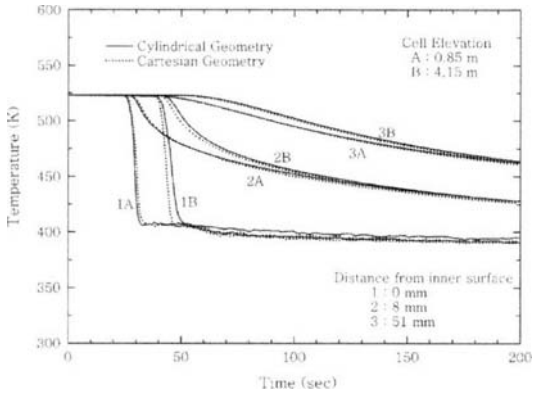

Fig. 9 Comparisons of temperature histories between cylindrical and cartesian coordinate

culation. It also seems that the temperature measurement error in experiment is one of the major factor in data difference.

Figure 9 shows the comparison of temperature history between Cartesian and Cylindrical coordinate calculation. It shows the same result for both coordinate systems except the small difference caused from different cell shape between Cartesian and Cylindrical coordinate modeling. Figure 10 shows the comparison of temperature history with different axial cell numbers of 12 and 19. It shows that calculation is not varying with different axial cell numbers. The 6 and 31 axial cell numbers are also tested and show same result. Hence the results show that there is no serious sensitivity occurred for different coordinates and axial cell numbers.

3.2 CCTF test

3.2.1 Comparisons of differential pressure and void fraction

Figure 11 shows the comparisons of differential pressures between the bottom and the top of the downcomer, that is, the downcomer water head. The friction loss is negligibly small comparing to the static water head in the downcomer since the water and the steam velocities are relatively small in the downcomer. The TRAC-M results show that the pressure differences about 80 sec after starting calculation has large oscillation since large condensation is occurred after LPCI injection started. Result also shows that TRAC-M over predict until about 180 sec after test started and under predict after that. The differential pressure of superheated downcomer wall temperature test shows lower level than that of saturated wall temperature test from around 120 sec after test started. This difference comes from the water level difference caused by void generation in the downcomer with superheated downcomer wall.

Figure 12 compares the downcomer void fractions both experiment in (a) and TRAC-M calculation in (b). Experimental data evaluated from measured differential pressures at several elevations for superheated and saturated wall temperature tests. Since the flow rates in the downcomer are relatively low, the differential pressures are due to the static water head only. The test begins with the downcomer empty, and the void fraction

is high everywhere which is shown in Fig. 12(a). After emergency core cooling (ECC) injection the void fractions decrease, starting with the elevations near the bottom of the downcomer. Of most interest are the void fraction comparisons higher in the downcomer. After 100 seconds, the void fractions for the saturated wall test decrease to lower values than those in the superheated wall test. This penalizes the core in two ways. First, the total static head in the downcomer is lower in the superheated wall test than in the saturated wall test, which reduced the core flooding rate. Second, as seen in Fig. 11, the core inlet subcooling is less in the superheated wall test than that in the saturated wall test, which decreases the core heat transfer.

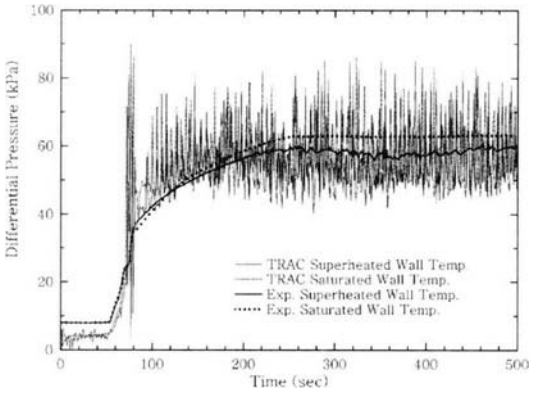

Fig. 11 Comparison of differential pressure at downcomer

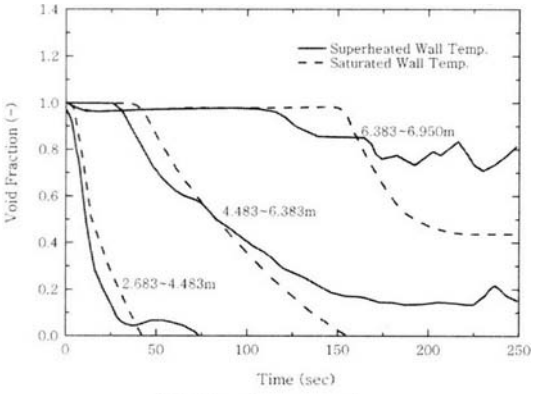

(a) Experiment results

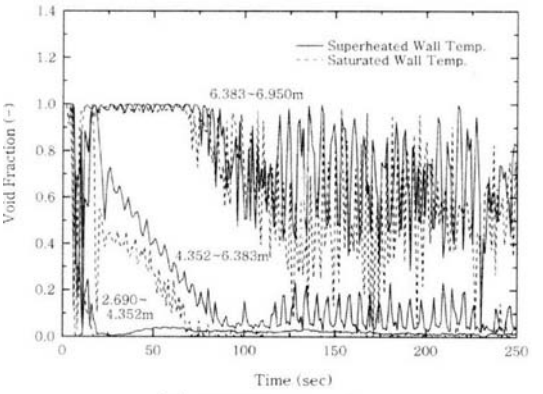

(b) TRAC-M results

Fig. 12 Comparison of void fraction at various elevation of the downcomer

3.2.2 Comparisons of the water mass collected in core

Figure 13 shows the comparison of the integration of core inlet mass flow for both tests. The mass flow rate of experimental result was evaluated by the mass balance calculation for the pressure vessel. The error of the evaluated core inlet mass flow rate was estimated to be about 15% at most. The result shows that the core inlet mass flow for the case of superheated wall is slightly lower than that of saturated wall temperature case in both experiment and calculation after about 130 sec even the difference is small. TRAC results shows less amount of water mass is collected after 220 sec in both cases, however they are in the range of the estimation error of the core inlet mass flow.

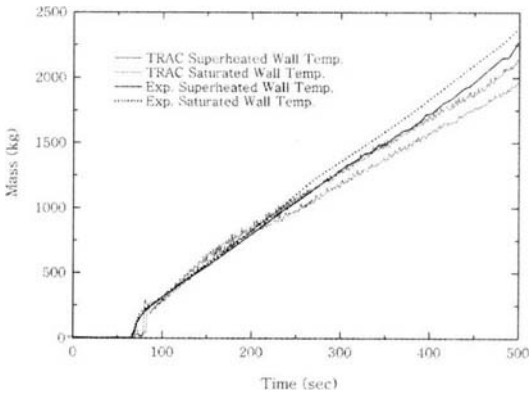

Fig. 13 Comparison of the water mass collected in core

3.2.3 Comparison of clad surface temperature

Figure 14 shows the comparison of the clad surface temperature histories between experiment and calculation. The maximum temperature curves of experimental data were obtained from the elevation of 2.44 m and the latest quench time curves were obtained from the elevation of 3.995 m from the bottom of heated section along an average power rod. The difference between experiment and calculation results is occurred in this figure, since TRAC-M data shown in this figure is not the temperature of exactly same location with that of experiment but the maximum temperature among the all of average power rods. It shows that the turnaround time and the maximum temperature at the same elevation are nearly same between superheated and saturated wall temperature tests in both calculation and experiment results. However, the average cladding surface temperature of superheated wall test is higher and the quench time in the superheated wall test is later than those of the saturated wall test. These are may caused by void generation of flooding water with downcomer boiling as already shown in Fig. 12. The increases in cladding temperature and quench time differences are small because of the relatively low initial core temperature in selected CCTF tests. Note that for an actual PWR, the clad temperatures following blowdown in the hot assembly are higher than those in CCTF. Hence the effects will be magnified as the clad temperatures increase and metal-water reaction also becomes important. The TRAC-M results over predict clad surface temperatures compare with experiment, however temperature history trends are the same.

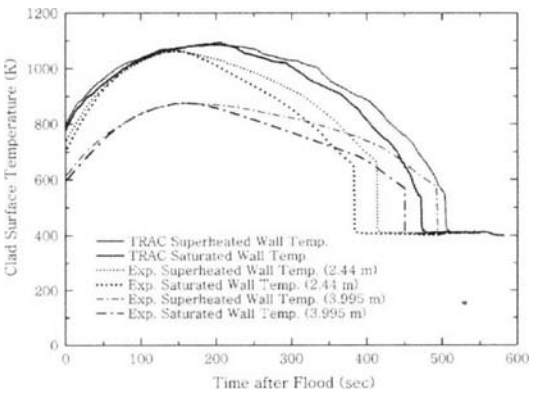

Fig. 14 Comparisons of clad surface temperatures

4. Conclusions

Downcomer boiling is the processes of subcooled and saturated boiling that may occur as fluid in the downcomer is brought to saturation by heat released from the core barrel, reactor vessel walls, and lower plenum metal. This process has recently been observed and become a concern as a new issue in the PWR large break LOCA analysis. Only two experimental tests were selected to verify an applicability of TRAC-M in downcomer boiling effects since experimental validation of downcomer boiling is highly limited.

From the present analytical study, the following conclusions were obtained :

From the downcomer effective water head test, the trends of temperature and pressure difference calculated using TRAC-M at various elevations agree well with that of experimental results. It also shows the decreasing of downcomer water head caused by downcomer boiling with high wall temperature of 250℃. The average values of calculated pressure difference are under predicted compare with experimental data at various locations. TRAC-M heat flux results show good agreement and are about 10% difference range compare with experimental results. The sensitivities of the code for different coordinate system and different axial nodding number are small. The results in downcomer effective water head test show that the TRAC-M calculates effective water head in downcomer conservatively, however the difference is small. Hence it can be concluded that the wall to liquid heat transfer analysis of TRAC-M is performed properly with current modeling for downcomer effective water head test.

TRAC-M results also show good agreements with the experimental results in downcomer

pressure difference, void fraction, core water mass flow and cladding surface temperature with CCTF test. Code predicted higher cladding temperature and later quenching time than the measured experimental data in CCTF experiments. Both experiment and calculation show the total static water head in the downcomer with the initial superheat temperature of the downcomer wall is lower than that of saturated, which reduce the core flooding rate. The core inlet subcooling is also less in the superheated wall test than that in the saturated wall test, which may decreases the core heat transfer. Those are caused by steam creation at the downcomer. The CCTF test results show that TRAC-M code tends to slightly underpredict differential pressure and void fraction in downcomer. It means that the current version of TRAC-M calculates downcomer boiling effects conservatively. However analysis results show large oscillations in differential pressure and void fraction due to the condensation. The effect of downcomer boiling on the core in current tests was a slight increase of the cladding temperature, and a delay of the quench time, however those effects will be magnified with an actual PWR.

The results of current research show that TRAC-M F90 Ver. 3.782 properly analyzes the effects of superheated downcomer wall temperature, which is related with downcomer boiling. And these show a slight conservative analysis trend. The downcomer boiling effects during reflood phase are captured in both of experiment and calculation results however the difference seems not highly significant. The database obtained in this research can be used for the future advanced analysis researches of the downcomer boiling.

References

Boyack, B. E., Lime, J. F., Pimentel, D. A., Spore, J. W. and Steiner, J. L., 1998, "TRAC-M/F77, Version 5.5, Developmental Assessment Manual," Los Alamos National Laboratory, *NUREG/CR-5673V2*.

Cappiello, M. W., 1989, "A Model for the Interfacial Shear in Vertical, Adiabatic Annular Mist Flow," Los Alamos National Laboratory document, *LA-CP-89-392*.

Hajime Akimoto, and Yoshio Murao, 1983, "Evaluation Report on CCTF Core-1 Reflood Test C1-2 (Run 11) and C1-3 (Run 12)," *JAERI-M 83-090*.

Spore, J. W., Elson, J. S., Jolly-Woodruff, S. J., Knight, T. D., Lin, J. C., Nelson, R. A., Pasamehmetoglu, K. O., Steinke, R. G., Unal, C., Mahaffy, J. H. and Murray, C., 2001, "TRAC-M/FORTRAN 90 (Version 3.0) Theory Mannual," Los Alamos National Laboratory, *NUREG/CR-6724*.

Steinke, R. G., Martinez, V., Schnurr, N. M., Spore, J. W. and Valdez, J. V., 2001, "TRAC-M/FORTRAN 90 (Version 3.0) User's Mannual," Los Alamos National Laboratory, *NUREG/CR-6722*.

Yukio Sudo and Hajime Akimoto, 1982, "Downcomer Effective Water Head during Reflood in Postulated PWR LOCA," *Journal of Nuclear Science and Technology*, 19, 1, pp. 34~45.

Yukio Sudo, Yoshio Murao, and Hajime Akimoto, 1980, "Experimental Results of the Effective Water Head in Downcomer during Reflood Phase of a PWR LOCA," *JAERI-M 8978*.